Potential Value of Apparent Diffusion Coefficient (ADC) in First-Line Treatment of Retinoblastoma

Paolo Galluzzi*

Neuroimaging and Neurointerventional (NINT) Unit, Azienda Ospedaliera e Universitaria Senese, c/o Policlinico S. Maria alle Scotte, Viale Bracci, Siena, Italy

*Corresponding Author: Paolo Galluzzi, Neuroimaging and Neurointerventional (NINT) Unit, Azienda Ospedaliera e Universitaria Senese, c/o Policlinico S. Maria alle Scotte, Viale Bracci, Siena, Italy.

Abstract

Background and Purposes: Assess the correlation between Apparent Diffusion Coefficient (ADC) values and prognostic parameters in retinoblastoma, including a possible contribution to prediction of response to intra-arterial chemotherapy (IAC).

Materials and Methods: Conventional MR images and ADC-maps in 38 retinoblastoma patients (23 males, 15 females, mean age 26.8 months, 4 group B, 2 group C, 15 group D, and 17 group E; ABC classification) were assessed. Echo Planar Imaging-Diffusion Weighted Imaging was performed before treatment with two B values (b 0 and 1000 s/mm^2), slice thickness 2.6 mm. Mean ADC-values in patients who underwent enucleation and those not-enucleated who underwent intra-arterial chemotherapy as first-line treatment were compared. ADC-values were correlated with tumor size and differentiation.

Results: Larger tumors showed lower ADC values. The difference in ADC-values between enucleated (mean= 880.7 x 10^{-6} mm^2/sec) and not enucleated patients (mean = 1026 x 10^{-6} mm^2/sec) was statistically significant (p = 0.002). A cut-off of 957.6 x 10^{-6} mm^2/sec may be suggested as a supplementary factor in discriminating tumors with different eye-survival prognosis (enucleation vs conservative treatment) (sensitivity 78%, specificity 66%, and accuracy 71%).

Conclusions: ADC may be taken in account when making a decision about the treatment of retinoblastoma. Although ADC alone is limited, and likely will be more useful clinically as a component in a multiparametric model.

Synopsis: ADC may be an adjunctive parameter to determine the best first-line treatment for a patient with retinoblastoma.

Keywords: Diffusion Weighted Imaging; Retinoblastoma; Therapy; Prognosis

Introduction

Retinoblastoma is the most common intraocular tumor in children [1]. Increasing eye preservation has been achieved by the introduction of conservative treatment strategies [2]. Recently, selective ophthalmic artery infusion of a chemotherapeutic agent has become available as first line treatment option for locally advanced disease in absence of glaucoma, massive vitreal dissemination, phthisis bulbi, anterior segment, corpus ciliaris, full-thickness choroidal, scleral and post-laminar optic nerve invasion [3,4]. As a consequence, more children are treated without histopathological confirmation of diagnosis or assessment of risk factors for disease dissemination and prognosis. High-resolution MRI is mandatory for pretreatment assessment, i.e. for diagnostic confirmation, detection of local tumor extent (particularly in order to evaluate whether tunics, anterior segment, corpus ciliaris, and optic nerve are involved or not); MRI is also useful in detection of associated developmental malformation of the brain and of associated intracranial tumors and metastasis [5,6]. In

2012 the European Retinoblastoma Imaging Collaboration (ERIC) group suggested a standardized MRI protocol in retinoblastoma for state-of-the-art pretreatment diagnostic imaging [7]. Other optional sequences may be added to the ERIC protocol, such as gradient echo T2 *or susceptibility weighted images (SWI), and Diffusion Weighted Imaging (DWI) with evaluation of the Apparent Diffusion Coefficient (ADC). To our knowledge, usefulness of ADC values in different first-line therapeutic settings (both conservative, such as the new developed intra-arterial chemotherapy (IA-CHT), and enucleation) has not been described. Hence, the purpose of this report is to investigate the correlation between ADC values, obtained in our patients with retinoblastoma, and both prognostic parameters and response to super selective IA-CHT.

Materials and Methods

Population

This study was performed in the Neuroradiological Unit of Siena Hospital (Italy). Between January 2011 and December 2015, patients with retinoblastoma were included in this study if they met the following criteria:

1. No treatment performed before MRI;
2. Enucleation or IA-CHT as first line treatment after MRI;
3. At least 12 month-follow up in patients treated with conservative therapy.

The population consisted of 48 patients (27 males, 21 females, average age 24.5, range 3 - 97 months). A total of three patients had bilateral disease: in that patients, the most affected eye was enucleated and evaluated in the ADC measurements.

MR protocol and ADC evaluation

All examinations were performed on a 1.5-T MR systems (Siemens Avanto, Erlagen, Germany), according to the protocol of ERIC [7]; affected eyes were examined using surface dedicated coil, positioned close to both eyes, after having put pads on the closed eyelids. Patients received 0.01 mmol/kg of body weight of gadolinium chelate (gadoterate dimeglumine, Dotarem, Guerbet, France). We added Echo Planar Imaging (EPI) SWI (FOV 100, thickness 1 mm, TR 46 ms, TE 38 ms, matrix 122 x 192) and DWI-sequences (b values: 0 and 1000 s/mm^2, FOV 230, thickness 2.6 mm, TR 3200 ms, TE 100 ms, matrix 192 x 192, diffusion directions 3). The total DWI acquisition time was 1.40 minutes. ADC measurements were performed by two observers independently (A.C and P.G.), respectively 18 and 28 years of experience in retinoblastoma imaging. ADC-values were extrapolated using a Region-of-Interest (ROI) method. On every slice in which the tumor was present, ROIs were hand-drafted on ADC maps for each affected eye; 1 to 5 ADC-values (depending on the tumor size) were obtained and mean values calculated (Figure 1). Mean ADC of the solid component of each tumor was obtained. Care was taken to avoid areas of high-signal on T2-weighted images (consistent with necrosis) and focal spots of signal void on SWI (consistent with calcifications); furthermore, areas showing absence of enhancement on post-contrast images were also excluded (Figure 2). For every single slice, a consensus was reached on the area that best excluded calcification and necrosis. The reliability of the ADC measurements was assessed by the intraclass correlation coefficient ICC [1,3] which was equal to 0.99, indicating the almost perfect concordance between the two neuroradiologists involved. Eyes highly distorted on DWI images because of intrinsic limits of EPI sequences were excluded to obtain reliable comparisons between ADC maps and SWI images in drawing ROIs: 10 eyes were excluded due to highly distorted images on dwi, so the final study population consisted of 38 patients (23 males, 15 females, average age 26.8, range 3 - 97 months).
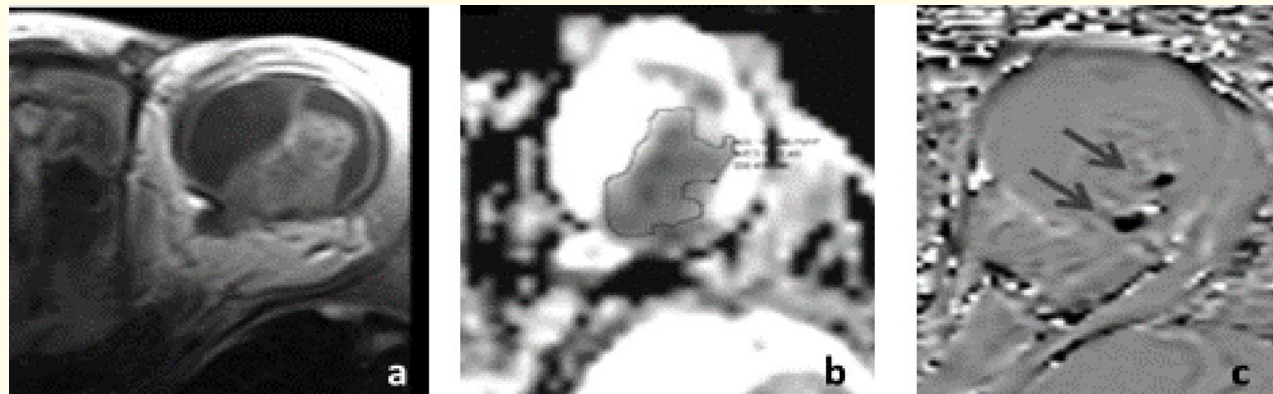
Figure 1: *5 month-old female with retinoblastoma. T1-weighted (a) image shows a large tumor mass in left eye. ADC map (b) of the affected eyes wash and-drafted avoiding calcifications, detectable as signal voids on SW images (arrows).*
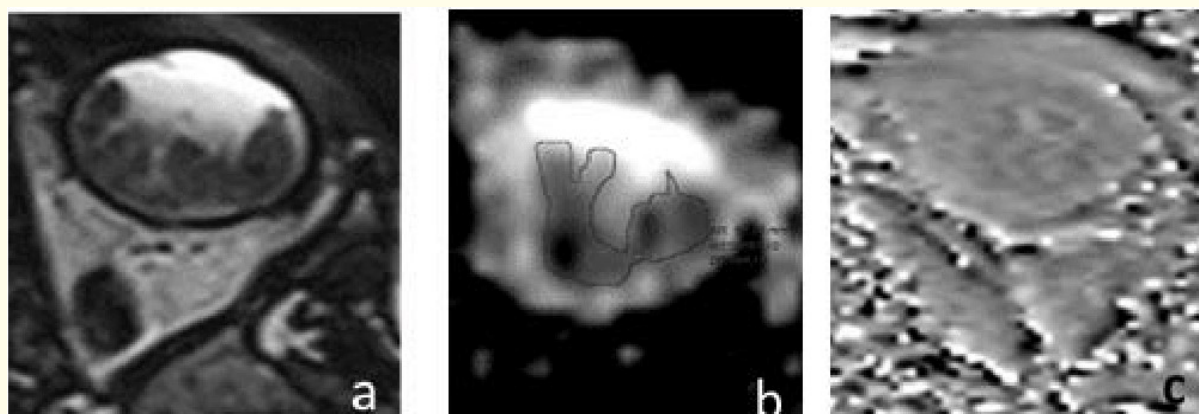

Figure 2: *45-month-old male with retinoblastoma. T2-weighted (a) ADC map (b and SW (c) images. ROIs were hand-drafted on ADC maps; SW image doesn't show calcifications.*

Final population was stratified in two subgroups according to therapy: 1) enucleation group (both as primary treatment or after failure of IAC), and 2) not-enucleated group (with at least 12 months without relapses at follow-up).

The treatment decision was based on both clinical and MRI findings: secondary glaucoma, anterior segment invasion, intravitreal hemorrhage, phthisis bulbi, and alerting signs at MRI (i.e. postlaminar invasion of the optic nerve, diffuse choroidal, corpus ciliaris and anterior segment infiltration, extraocular intraorbital dissemination) are the criteria that our Oncologic Multidisciplinary Group have chosen to proceed to enucleation of the affected eye.

Clinical records were reviewed by one reviewer (D.R.) to assess age at diagnosis, laterality, ABC, groups according to the international ABC classification [8], treatment and follow-up. ABC classification divides retinoblastoma in 5 progressive higher risk groups (A to E) (i.e. A stands for very low risk, and E for very high risk) (Table 1).

Group	Subgroup	Quick reference	Specific features
A	A	Small tumour	Retinoblastoma < 3 mm in size
B	B	Larger tumour	Retinoblastoma > 3 mm in size or
		Macula	Macular retinoblastoma location (< 3 mm to foveola)
		Juxtapapillary	Juxtapapillary retinoblastoma location (< 1.5 mm to disc)
		Subretinal fluid	Clear subretinal fluid > 3 mm from macula
C		Focal seeds	Retinoblastoma with
	C1		Subretinal seeds < 3 mm from retinoblastoma
	C2		Vitreous seed < 3 mm from retinoblastoma
	C3		Both subretinal and vitreous seeds < 3 mm. from retinoblastoma
D		Diffuse seeds	Retinoblastoma with
	D1		Subretinal seeds > 3 mm from retinoblastoma
	D2		Vitreous seeds > 3 mm from retinoblastoma
	D3		Both subretinal and vitreous seeds > 3 mm from retinoblastoma
E	E	Extensive retinoblastoma	Extensive retinoblastoma occupying > 50% globe or
			Neovascular glaucoma
			Opaque media from haemorrhage in anterior chamber, vitreous, or subretinal space
			Invasion of postlaminar optic nerve, choroid (2 mm), sclera, orbit, anterior chamber

Table 1: *International Classification of Retinoblatoma.*

MRI findings of suspected optic nerve, choroid, sclera, corpus ciliaris, and anterior segment infiltration were correlated with histology in eyes enucleated as first line treatment.

This study was conducted in accordance with recommendations of the local ethics committee, with waiver of informed consent.

Histological assessment

Histopathological examination was performed on all enucleated eyes according to international guidelines [9] by local pathologist (P.T., 35 years of experience in retinoblastoma), who was blinded to both patient clinical records and MR findings. Staging was assigned according to pTNM classification. Histopathological evaluation, by using H&E staining, included the assessment of the degree of tumor differentiation. Therefore, our cases were stratified in three groups: totally undifferentiated tumors (without Flexner-Wintersteiner rosettes), poorly-differentiated tumors (defined by the presence of spare rosettes), and differentiated tumors (defined by the presence or many rosettes).

Statistical analysis

A commercially available software (MATLAB version 7.5.0.342-R2007B) was used. Normality and homoscedasticity were verified using Shapiro Wilk test; if verified, we applied Student-t test, reporting average values and standard deviation (SD); if not verified, non-parametric Mann-Whitney test was applied to compare 2 groups, reporting median values and interquartile range (IQR). To compare 3 or more groups ANOVA Kruskal-Wallis test was used. A p-value < 0.05 was considered significant.

Particularly, Student-t test was used to compare mean ADC values in eyes that had been enucleated vs not enucleated ones and to compare mean ADC values between undifferentiated and moderately differentiated tumors. A Receiver Operating Characteristic (ROC) curves were also used.

Mann-Whitney test was used a) to compare ADC values between eyes that had been enucleated after IA-CHT and not-enucleated eyes; b) to compare ADC values between eyes that had been enucleated at diagnosis and after IA-CHT.

Results

Clinical findings

According to the ABC classification [8], there were 4 eyes in group B, 2 eyes in group C, 15 in group D, and 17 in group E.

14 eyes (all group B) were enucleated as first treatment after diagnosis (mean interval between MRI and enucleation: 5.7 days); In 24 eyes IA-CHT with melphalan as first line therapy was performed; among these patients, 5 (all group D) underwent enucleation because of complications or persistence/progression of the disease. The remaining 18 eyes had good response to IAC at a follow-up of at least 12 months. No patients presented extra-ocular disease at follow-up.

Correlation between ADC and size

Tumors were divided in three groups, according to the maximum diameter: small size (< 10 mm; n = 3), medium size (10 - 15 mm, n = 17), and large size (> 15 mm, n = 18). We didn't find any significant difference in ADC values among the 3 groups (KW = 5.8; p = 0.053), although large tumors showed lower ADC values (Figure 3).
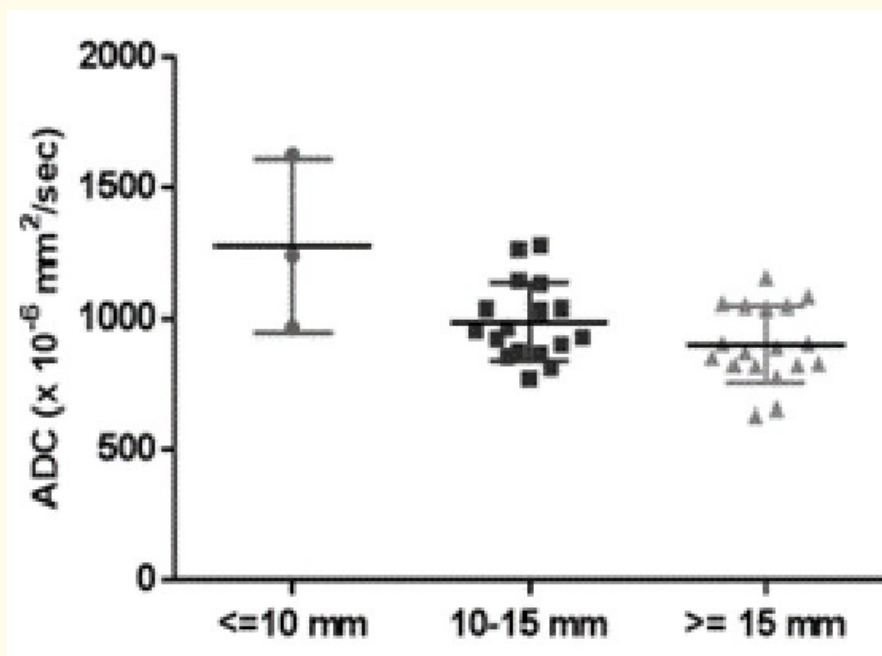

Figure 3: Mean ADCs of small, medium, and large size tumors.

ADC-histopathological grading and Correlation between MRI findings and histology

7 out of 14 eyes enucleated at diagnosis contained totally undifferentiated tumors, and 7 poorly-undifferentiated tumors. No differentiated tumor was found. In 12 out of 14 eyes optic nerve infiltration was identified; in 6 out of 14 eyes choroidal infiltration was appreciable (Table 2).

Suspected infiltrations at MRI Infiltrations at histology (TP)	No infiltrations at MRI No infiltrations at histology (TN)	Suspected infiltrations at MRI No infiltrations at histology (FP)	No infiltrations at MRI Infiltrations at histology (FN)
12 ON	1	1 ON	1 ON
5 CH		3 CH	1 CH
			2 SCL

Table 2: Correlation between MRI findings and histology.

ON: Optic Nerve; CH: Choroid; SCL: Penetrating Scleral Vessel(s)

ADC-values in poorly-differentiated tumors were statistically lower (776,1 x 10-6 mm²/sec; SD: 105.8) than that of undifferentiated tumors (839.9 x 10-6 mm²/sec; SD: 77.69) (T (12) = 2.37; p = 0.03).

Correlation between ADC-values and therapeutic outcome

In our population, mean ADC was 969.2 x 10-6 mm²/sec (range 630-1625). ADC-values determined by both observers resulted in an intraclass correlation of 0.91. Mean ADCs for each tumor are summarized in table 3.

PN	Outcome	Mean ADC x 10⁻⁶ mm²/sec	ABC	pTNM	Largest MRI diam. (mm)
10	E (NT)	630	E	pT2a	17.0
31	E (NT)	657	E	pT2a	17.7
36	E (NT)	769	E	pT2a	14.4
12	E NT)	775	E	pT4b	17.0
13	E (NT)	810	E	pT2a	13.6
23	E (NT)	819	E	pT2a	15.0
26	E (NT)	822	E	pT3b	15.5
37	E (AT)	822	D	pT1	15.0
32	CT	829	E		17.8
27	E (NT)	852	E	pT3a	18.6
7	CT	855	D		12.2
20	CT	868	B		13.8
30	CT	873	D		16.1
38	E (NT)	877	E	pT3a	14.6
14	E (NT)	890	E	pT3a	17
34	CT	902	D		14.3
24	E (NT)	905	E	pT3a	18.9
8	E (NT)	906	E	pT2a	17.3
21	CT	924	D		14.0
17	E (NT)	931	E	pT2b	14.6
4	E (AT)	955	D	pT1	11.0
9	CT	966	D		14.2
25	CT	968	D		10.0
18	CT	1030	D		12.0
11	CT	1038	C		11.7
3	E (AT)	1039	D	pT1	13.2
15	CT	1039	D		18.3
35	E (NT)	1047	E	pT2b	16.0
6	CT	1048	E		18.0
19	CT	1055	D		15.5
16	E (AT)	1083	D	pT1	15.7
22	CT	1132	E		14.0
5	E (AT)	1144	D	pT1	14.6
33	CT	1156	C		15.2
28	CT	1242	B		8.5
29	CT	1266	B		13.0
1	CT	1281	D		10.4
2	CT	1625	B		10.0

Table 3

PN: Patient Number; CT: Conservative Treatment; E: Enucleated; AT: After Treatment; NT: No Treatment

Mean ADC-values in not enucleated group were significantly higher (mean = 1026 x 10^{-6} mm^2/sec; SD = 143.1; p = 0.002) in comparison to enucleated group (mean = 880.7 x 10^{-6} mm^2/sec; SD = 134.5; p = 0.002). A cut-off of 957.6 x 10^{-6} mm^2/sec between the two groups was found (sensitivity 78%, specificity 66%, accuracy 71%) (Figure 4 and 5).

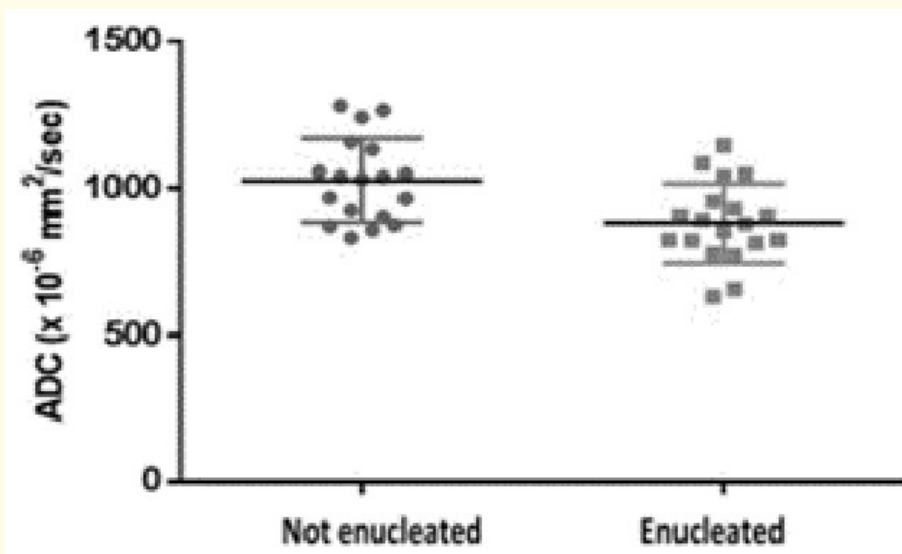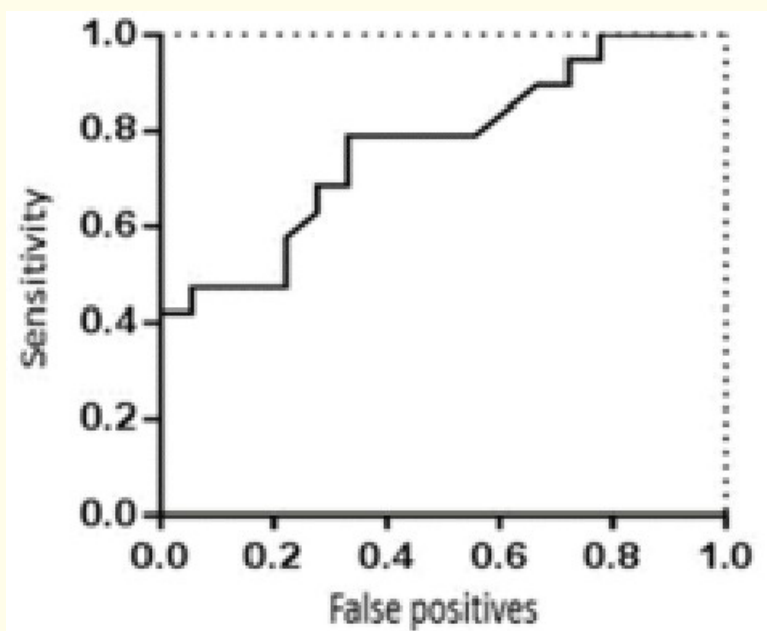***Figure 4:*** *Mean ADC of enucleated and not enucleatec patients.*

Figure 5: *ROC: a cut-off of 957,6x10-6 mm^2/sec gives sensitivity 78%, specificity 66%, accuracy 71%.*

Discussion

DWI and the resulting ADC maps can evaluate water diffusion in a tissue, and they are strictly correlated to its molecular and cellular architecture. Our study showed the potential role of DWI in the evaluation of retinoblastoma patients.

The increasing use of conservative treatment strategies in retinoblastoma leads to an increasing number of children treated without histologic reports.

Recently, DWI and ADC have been proposed as prognostic marker in many tumors, including tumors of the orbit [10-14]. Sepahdari., *et al*. reported that malignant tumor of the orbit (such as lymphoma, rhabdomyosarcoma, melanoma, and metastasis) have lower average ADC value in comparison to benign lesions [11]. These findings were confirmed by Razek., *et al*. [12] and de Graaf., *et al* [13].

In our paper we correlated ADC values with tumor size. It has been reported that larger tumors tend to be more aggressive [15]. Recently, Yan., *et al*. demonstrated that also smaller tumors (6 - 10 mm) can lead to sparse orbital and optic nerve invasion [16]. In our series, larger tumors tended to have lower ADC values, supporting the results reported by Razek., *et al*. [12]. However, we didn't find statistically significant difference in ADC-values between small (< 10 mm), medium (10 - 15 mm), and large (> 15 mm) tumors. This could be due to the limited number of patients with small tumors in our cohort.

In retinoblastomas, undifferentiated tumors are composed of densely packed cells, while tumor cells in differentiated retinoblastomas are clustered in a specific pattern, called Flexner-Wintersteiner rosettes, and display a relatively paucicellular cytoarchitecture. It is well known that high cellularity tissues show lower ADC-values in comparison to low cellularity and necrotic tissues [11]. Undifferentiated tumors usually show lower ADC than more differentiated ones [10], as confirmed in our study.

In our series, mean ADC in the tumor was 969.2 x 10^{-6} mm^2/sec (range 630-1625). Our results are in agreement with recently published series by de Graaf., *et al*. [13] (1030, range 720 - 1220), Sepahdari., *et al*. [17] (930 +/- 300), and Chen., *et al*. (940 + 24) [14], but they are higher than what reported by Razek., *et al*. [12] (490, range 200 - 860). This difference may be due to the sensitivity of ADC values to many different factors (field strengths, manufacturer, sequences, artifacts etc.) and lack of reproducibility, but also to the presence or absence of calcifications in the ROIs. Razek., et al. included intra-tumoral calcific areas in their measurements (possibly leading to lower ADC value), while calcifications were excluded in our measurements on the basis of T2-weighted, SWI and T1-weighted contrast-enhanced images. The addition of composite Susceptibility Weighted images (both phase and magnitude) to exclude areas of calcifications could increase the reliability of area for ADC evaluations.

ADC evaluation may add to already known criteria used to choose the proper treatment (conservative or enucleation) in each case, and to the chances of predicting tumor response in the conservative group. Currently, indications to enucleation are based on clinical (bilaterality, heredity), ophthalmoscopic (secondary glaucoma, anterior chamber tumor, iris neovascularization, vitreal hemorrhage, phthisis bulbi) and neuroradiological (retro-laminar optic nerve invasion, massive extension to the uvea and the sclera) risk factors [18-21]. In the present study, enucleated eyes showed metastatic risk factors on conventional MR imaging that contributed to the decision of enucleating as first line treatment; moreover, ADC-values in patients that had been enucleated were significantly lower than that in patients that had been treated conservatively.

In our series, mean ADC value 957.6 x 10^{-6} mm^2/sec was suggested as a cut-off to discriminate tumors which may be more responsive to IA-CHT and tumors which more probably will require enucleation as first line treatment or after failure of one or more conservative treatments.

In patients that received a conservative treatment we didn't find significant differences in mean ADCs between those with good outcome (i.e. no relapses at 12-months follow-up) and those with failure. This can be due to the small number of case in the failure group (i.e.

5). However, we found a significant difference between mean ADCs of patients enucleated at diagnosis and those enucleated after therapy. Additionally, the eyes enucleated at diagnosis presented significantly lower mean ADCs than both patients not enucleated and enucleated after therapy. It's interesting that all patients enucleated at diagnosis were in group E according to ABC Classification, while all patients enucleated after IA-CHT were in group D, and didn't show clinical-neuroradiological risk factors for extra-ocular invasion (histological evaluation pT1).

Some limitations of our study should be addressed

First, the sample size was too small to allow us to assess the possible correlation between ADC-values and both tumor size and degree of tumor differentiation. Furthermore, in our limited series, mean ADC value 957.6 x 10^{-6} mm^2/sec was suggested as a cut-off because it guaranteed the best compromise among statistical parameters (i.e. sensitivity 78%, specificity 66%, and accuracy 71%). Further studies with a larger cohort of patients, preferentially in a multicenter study and with a longer follow-up time, are required to confirm our data, since the accuracy is not particularly high. Then, we did not obtain histological assessment in all eyes; however, enucleation after therapy can lead to different histological patterns, and be not comparable with pathological assessment in eyes enucleated at diagnosis. Another shortcoming is the possible bias in the ROI measurement: in very small lesions, we have to consider the partial volume artifact due to the vitreal fluid. Anyway, we obtained a good interclass correlation coefficient between the two observers. Another limitation might be the availability of surface coils and/or high field magnets, required to obtain thin DWI images, in larger treatment centers. Finally, the sensitivity and specificity of ADC values don't appear high enough to be successfully applied in clinical management of retinoblastoma without considering a multiparametric model including other MRI-derived findings.

Conclusion

ADC may represent an additional prognostic parameter in the management of patients with retinoblastoma, by predicting the degree of tumor cellularity, possibly correlating with tumor histology.

Thus, the potential for DWI-ADC to noninvasively assess prognostic and predictive marker in retinoblastoma tumors is promising and warrants further investigation, based on the current data ADC will need to be consider with other imaging findings to differentiate aggressive/resistant tumors from those potentially responding to the therapy, and to early differentiate responder vs. non-responder patients during conservative treatments.

Bibliography

1. Rodriguez-Galindo C., et al. "Retinoblastoma". *Pediatric Clinics of North America* 62.1 (2015): 201-223.

2. Lumbroso-Le Rouic L., *et al.* "Conservative treatments of intraocular retinoblastoma". *Ophthalmology* 115.8 (2008): 1405-1410.

3. Abramson DH., *et al.* "Superselective ophthalmic artery chemotherapy as primary treatment for retinoblastoma (chemosurgery)". *Ophthalmology* 117.8 (2010): 1623-1629.

4. Abramson DH. "Retinoblastoma: saving life with vision". *Annual Review of Medicine* 65 (2014): 171-184.

5. de Graaf P., *et al.* "Contrast-enhancement of the anterior eye segment in patients with retinoblastoma: correlation between clinical, MR imaging, and histopathologic findings". *American Journal of Neuroradiology* 31.2 (2010): 237-245.

6. Lemke AJ., *et al.* "Retinoblastoma: MR appearance using a surface coil in comparison with histopathological results". *European Radiology* 17.1 (2007): 49-60.

7. Pim de Graaf., *et al.* "Guidelines for imaging retinoblastoma: imaging principles and MRI standardization". *Pediatric Radiology* 42.1 (2012): 2-14.

8.   Murphree AL. "Intraocular Retinoblastoma: the Case for a New Group Classification". *Ophthalmology Clinics of North America* 18.1 (2005): 41-53.

9.   Sastre X., *et al*. "Proceedings of the consensus meetings from the International Retinoblastoma Staging Working Group on the pathology guidelines for the examination of enucleated eyes and evaluation of prognostic risk factors in retinoblastoma". *Archives of Pathology and Laboratory Medicine* 133.8 (2009): 1199-1202.

10.   Abdel Razek AA., *et al*. "Differentiation between benign and malignant orbital tumors at 3-T diffusion MR imaging". *Neuroradiology* 53.7 (2011): 517-522.

11.   Sepahdari AR., *et al*. "Indeterminate orbital masses: restricted diffusion at MR Imaging with echo-planar Diffusion-weighted Imaging Predicts Malignancy". *Radiology* 256.2 (2010): 554-564.

12.   Abdel Razek AA., *et al*. "Correlation of apparent diffusion coefficient at 3T with prognostic parameters of retinoblastoma". *American Journal of Neuroradiology* 33.5 (2012): 944-948.

13.   de Graaf P., *et al*. "Single-shot turbo spin-echo diffusion-weighted imaging for retinoblastoma: initial experience". *American Journal of Neuroradiology* 33.1 (2012): 110-118.

14.   Chen S., *et al*. "The value of MRI in evaluating the efficacy and complications with the treatment of intra-arterial chemotherapy for retinoblastoma". *Oncotarget* 8.24 (2017): 38413-38425.

15.   Shields CL and Shields JA. "Diagnosis and management of retinoblastoma". *Cancer Control* 11.5 (2004) : 317-327.

16.   Yan J., *et al*. "Establishment of the relationship between tumor size and range of Histological Involvement to Evaluate the rationality of current retinoblastoma management". *PLOS ONE* 8.11 (2013): e80484.

17.   Sepahdari AR., *et al*. "Diffusion-weighted imaging of malignant ocular masses: initial results and directions for further study". *American Journal of Neuroradiology* 33.2 (2012): 314-319.

18.   Galluzzi P., *et al*. "MRI helps depict clinically undetectable risk factors in advanced stage retinoblastomas". *Neuroradiology Journal* 28.1 (2015): 53-61.

19.   Aerts I., *et al*. "Results of a multi center prospective study on the postoperative treatment of unilateral retinoblastoma after primary enucleation". *Journal of Clinical Oncology* 31.11 (2013): 1458-1463.

20.   Shields CL., *et al*. "The international Classification of Retinoblastoma predicts chemoreduction success". *Ophthalmology* 113.12 (2006): 2276-2280.

21.   Suzuki S., *et al*. "Selective ophthalmic arterial injection therapy for intraocular retinoblastoma: the long-term prognosis". *Ophthalmology* 118.10 (2011): 2081-2087.